



Removal of m-phenylene diamine by adsorption onto activated carbon: kinetics, equilibrium and process design

Isha Patel, Manali Rathod, Kalpana Mody, Shaik Basha*

Discipline of Marine Biotechnology and Ecology, CSIR-Central Salt & Marine Chemicals Research Institute, Bhavnagar 364 002, Gujarat, India, Tel. +91 278 2561354; Fax: +91 278 2570885; emails: ishapatel51@yahoo.co.in (I. Patel), mi_212@yahoo.co.in (M. Rathod), khmody@csmcricri.org (K. Mody), sbasha@csmcricri.org (S. Basha)

Received 14 August 2014; Accepted 17 November 2014

ABSTRACT

The adsorption behavior of m-phenylene diamine (m-PDA) from aqueous solution onto activated carbon was investigated under various experimental conditions, such as contact time, adsorbate concentration, and temperature. Maximum adsorption capacity for m-PDA was found to be 33.17 mg g⁻¹ at pH 7.0 and temperature 303 K. The adsorption kinetics data were best described by the pseudo-second-order rate equation and the equilibrium was achieved after 120 min. The m-PDA adsorption was governed by film diffusion process. Besides, equilibrium data were very well represented by the Redlich–Peterson model. A model for prediction of the dose of adsorbent required to achieve a range of m-PDA removals for a given number of adsorption–desorption cycles has been developed and validated based on the Langmuir isotherm. Thermodynamic parameters indicated the spontaneous, endothermic, and increased random nature of m-PDA adsorption. The amide, carboxylic acid, and nitro groups of the activated carbon were involved in chemical interaction with the m-PDA molecules. Results suggested that the activated carbon has good potential for remediation of m-PDA contaminated waters.

Keywords: Activated carbon; Adsorption; m-phenylene diamine; Kinetics; Thermodynamics

1. Introduction

Aromatic amines are environmental pollutants and evident in wastewaters of various industries such as textiles, dyes, pesticides, soaps and detergents, surfactants, iron and steel, resins and plastics, petroleum refining, and coal conversion [1,2]. Many of the aromatic amines and their derivatives are potential carcinogenic and mutagenic agents [3–5]. In addition, aromatic amines also have relatively high biological oxygen demand, and therefore, when present in

sufficient concentrations can greatly reduce or deplete the dissolved oxygen in surface water. Therefore, removal of these compounds from water and wastewater is of great significance.

The aromatic amine, m-phenylenediamine (also known as 3-aminoaniline; 1,3-benzenediamine; 1,3-diaminobenzene) is a chemical intermediate used for manufacturing dyes, thin-film composite membrane, aramid fiber, and in photography and medical applications. Meta phenylene diamine (m-PDA) has two amino groups attached to a benzene ring, at meta position, with respect to each other. Properties which make m-PDA so versatile are its fire resistance,

*Corresponding author.

excellent chemical and temperature stability, and fast cure. The demand for m-PDA is growing rapidly with increase in application of engineering materials, especially aromatic polyamide fibers and polyurethane [6]. If released to water, m-PDA is expected to be adsorbed by hazardous sediment and suspended solids in the acidic environment [7,8]. Though m-PDA is not readily biodegradable, it may be removed by biodegradation under specific conditions involving acclimatized micro-organisms.

The removal of aromatic amines can be achieved by several techniques such as adsorption, microbial chemical oxidation, advanced oxidation processes, and electrochemical techniques [9,10]. However, adsorption methods are more effective due to their cost-effectiveness, effective treatment in dilute solutions, high uptake capacity, faster regeneration kinetics, and greater selectivity [11]. In this regard, many adsorbents including pyrolusite and activated carbon [12], oxygenated activated carbon [13], montmorillonite-Ce-phosphate compound [2], beta-cyclodextrin-based polymers [14], phenyl-functionalized mesoporous silica [15] have been investigated in recent years for sorption of aromatic amines.

In the present work, the removal of m-PDA from water has been exhaustively studied using a highly porous and high surface area-activated carbon. The mechanisms of adsorption as well as the influence of several factors (contact time, pollutant concentration, temperature, and pH of the solution) on the adsorption process were thoroughly investigated. A model describing the process of wastewater treatment by multiple cycles of adsorption–desorption has been developed and validated.

2. Experimental

2.1. Materials

The chemicals used in this study were of analytic reagent grade, m-PDA ($C_6H_8N_2$, CAS No. 108-45-2, FW: 108.12) were procured from Sigma and used without further purification. The m-PDA stock solutions were prepared by dissolving accurately weighed m-PDA in Millipore water to the concentration of $1,000\text{ mg L}^{-1}$. The experimental solutions were obtained by diluting the m-PDA stock solutions in accurate proportions to different initial concentrations. In order to obtain the m-PDA solution of different initial pH, infinitesimal amount of 1 M HCl or 1 M NaOH (S.D. Fine Chem, India) were added. Activated carbon (AC) of 100–400 mesh size was purchased from Thermo-Fisher, India. The physicochemical properties of the precursor are listed in Table 1.

2.2. Batch adsorption experiments

All the experiments were conducted at a constant temperature of $25 \pm 1^\circ\text{C}$ to produce environmentally relevant conditions except thermodynamic experiments. The effect of solution pH on the equilibrium uptake of m-PDA from aqueous solution by activated carbon was investigated between pH 2 and 10 by adjusting with HCl and NaOH solutions. The experiments were performed by adding a known weight of adsorbent into 250 mL Erlenmeyer flasks containing 250 mg L^{-1} of m-PDA. The flasks were stirred at 140 rpm and 298 K for 24 h to attain equilibrium, and the amount of m-PDA remaining in solution was measured by a high-performance liquid chromatography (HPLC) system after the separation of adsorbent by membrane filtration (Millipore 0.45 mm pore size).

The adsorption kinetic studies were conducted using 250 mL of m-PDA solution with initial concentration of 265.5 mg L^{-1} . The samples were withdrawn periodically and the residual concentration of m-PDA in the aqueous phase was analyzed after membrane filtration.

Initial concentration experiments were carried out in 250 mL flasks containing m-PDA solution (100 mL) of known concentrations ($25\text{--}150\text{ mg L}^{-1}$). Weighed amounts of AC (400 mg) were added to each flask and the mixture was agitated on the rotary shaker. After 24 h of agitation, the solution was separated from the biomass by membrane filtration and analyzed by HPLC. The effect of dye sorption by the membrane filter during the filtration process was minimized by discarding the first 25 mL portion of the m-PDA solution. The remnant was used for the measurement of m-PDA concentration.

m-PDA control solutions were also filtered using the same procedure and the concentration was ascertained. The m-PDA concentration of the control was used as the initial concentration for calculating the quantity of m-PDA transferred from the solution to the sorbent. The adsorption experiments were conducted in replicate (at a minimum $n = 2$) with two controls. The average values were used in the study for clarity (without error bars being included in the Figures), as the reproducibility of repeated runs was found to be within an acceptable limit ($\pm 5\%$). Controls were employed to ensure that sorption was by AC only, and any effect of sorption of m-PDA onto the wall of the reaction bottles could be eliminated.

2.3. Analysis

The concentration of m-PDA was determined by HPLC system consisting of a Shimadzu Prominence

Table 1
Physicochemical characteristics of activated carbon

Parameter	Activated carbon
Carbon content (%)	72.34
Hydrogen content (%)	3.28
Nitrogen content (%)	0.69
Oxygen content (%)	23.05
Sulfur content (%)	0.54
<i>Surface area</i>	
Single point surface area at P/P_0 0.203, $\text{m}^2 \text{g}^{-1}$	266.2
BET surface area, $\text{m}^2 \text{g}^{-1}$	258.73
BJH adsorption cumulative surface area of pores between	17.87
BJH desorption cumulative surface area of pores between 1.7 and 300 nm diameter, $\text{m}^2 \text{g}^{-1}$	37.98
<i>Pore volume</i>	
Single point adsorption total volume of pores less than 75.69 nm at P/P_0 0.973, $\text{cm}^3 \text{g}^{-1}$	0.124
<i>Pore size</i>	
Adsorption average pore diameter (4 V/A by BET), nm	1.92
BJH adsorption average pore diameter (4 V/A), nm	3.45
BJH desorption average pore diameter (4 V/A), nm Å	2.59

(Shimadzu Corporation, Japan) low-pressure gradient pump equipped with a UV-visible detector. A 150×4.6 mm, $3.5 \mu\text{m}$ particle enable C18H column was used for separation of the analyte. The wavelength of the detector was set at 254 nm. Mobile phase consisted of 80% acetonitrile to 20% water and it was filtered by nylon filters and degassed by ultrasonication for 30 min. The eluent flow rate was 1.5 mL min^{-1} with injection volume $50 \mu\text{L}$. The quantitative determination of m-PDA was performed using an external standard, and the calculations were based on the average peak areas of the standard. The data were processed using LC solution software.

The amount of m-PDA sorbed at equilibrium, q_e (mg g^{-1}) which represented the m-PDA uptake, was calculated from the difference in dye concentration in the aqueous phase before and after adsorption, as per following equation:

$$q_e = \frac{V(C_i - C_e)}{W} \quad (1)$$

where V is the volume of dye solution (L), C_i and C_e are the initial and equilibrium concentrations of m-PDA in solution (mg L^{-1}), respectively, and W is the mass of activated carbon (g).

2.4. Nonlinear regression analysis

All the model parameters were evaluated by nonlinear regression using DATAFIT[®] software (Oakdale

Engineering, USA). The optimization procedure required an error function to be defined in order to be able to evaluate the suitability of the equation to the experimental data. Apart from the regression coefficient (R^2), the residual or sum of square error (SSE) and the standard error (SE) of the estimate were also used to gauge the goodness-of-fit. SSE can be defined as:

$$\text{SSE} = \sum_{i=1}^m (Q_i - q_i)^2 \quad (2)$$

SE can be defined as:

$$\text{SE} = \sqrt{\frac{1}{m-p} \sum_{i=1}^m (Q_i - q_i)^2} \quad (3)$$

where q_i is the observation from the batch experiment i , Q_i is the predicted value from the isotherm for corresponding q_i , m is the number of observations in the experimental isotherm, and p is the number of parameters in the regression model. The smaller SE and SSE values indicate the better curve fitting.

2.5. FTIR, SEM, and EDX studies

Infrared spectra of unloaded and m-PDA loaded activated carbon were obtained using a Fourier Transform Infrared Spectrometer (FTIR GX 2000, Perkin-Elmer). For the FTIR study, 30 mg of finely

ground biomass was palletted with 300 mg of KBr (Sigma) in order to prepare translucent sample disks. The FTIR spectra were recorded with 10 scans at a resolution of 4 cm^{-1} .

The surface structure of activated carbon was analyzed by scanning electron microscopy (SEM) using JEOL 5600 LV SEM. Unloaded and m-PDA loaded activated carbon samples were mounted on a stainless steel stab with a double-stick tape followed by sputter-coating gold to improve conductivity to increase the electron conduction and to improve the quality of the micrographs.

3. Results and discussion

3.1. Effect of solution pH

Solution pH is one of the important factors that control the adsorption process of organic compounds on carbon materials because it controls the electrostatic interactions between the adsorbent and the adsorbate [16]. The effect of initial pH on the adsorption of m-PDA on to activated carbon was examined for pH values ranging from 3 to 13 (Fig. 1). The equilibrium sorption capacity was minimum at pH 3 (15.42 mg g^{-1}) and increased up to pH 5 (31.74 mg g^{-1}), then remained nearly constant (30.94 mg g^{-1}) over the initial pH of the range 5–7. At solution $\text{pH} < 5$, the sorption capacity was low as the adsorbent was positively charged, and m-PDA molecule was either neutral or partially positively charged. At this acidic pH, the amine groups of the m-PDA were almost protonated. If electrostatic interaction was the only mechanism for

the m-PDA adsorption, then the sorption capacity should be at a maximum within the range $\text{pH } 5\text{--}7$. In this pH range, the surface of activated carbon is positively charged ($\text{pH}_{\text{pzc}} = 9.0$) and m-PDA is negatively charged (pK_a of m-PDA 5.1) [17]. The protonated groups of activated carbon were mainly carboxylic, phenolic, and chromenic groups [15,18,19], while the deprotonated groups of the m-PDA were probably the amine groups. The constant adsorption capacity of activated carbon for m-PDA over the pH range 5–7 was an indication that the electrostatic mechanism was not the only mechanism for m-PDA adsorption in this system. Activated carbon can also interact with m-PDA molecules by hydrogen bonding and hydrophobic interaction through the polar functional groups (e.g. $-\text{COOH}$; H-donor) and amino groups (H acceptor) [20,21]. The reduction in m-PDA adsorption at highly basic conditions ($\text{pH } 11\text{--}13$) can be attributed to electrostatic repulsion between the negatively charged activated carbon and the deprotonated m-PDA molecule.

3.2. Adsorption kinetics

The effect of contact time on the adsorption of m-PDA onto activated carbon was studied in the concentration range $50\text{--}100\text{ mg L}^{-1}$ (Fig. 2). The equilibrium time was found to be 150 min. The adsorption was higher in the beginning due to greater number of reaction sites available for the adsorption of m-PDA. Consequent to the increase in initial m-PDA concentration from 50 to 100 mg L^{-1} , the adsorption capacity increased from 19.72 to 31.78 mg g^{-1} , indicating that

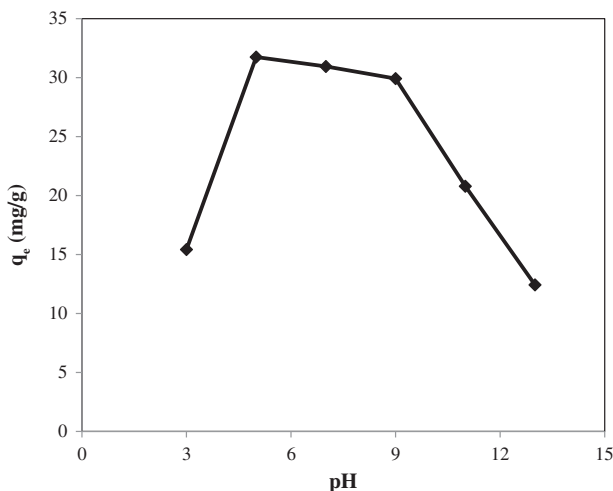


Fig. 1. Effect of pH on adsorption capacity of activated carbon (initial concentration of 100 mg L^{-1} and solid to liquid ratio (s/l) of 1.6 g L^{-1}).

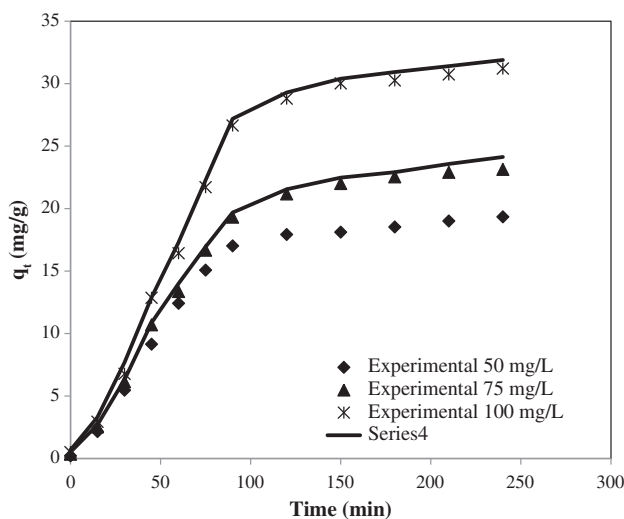


Fig. 2. Comparison of the experimental (legends) and the model plots of pseudo-second order kinetics (lines) ($\text{pH } 7.0$ and solid to liquid ratio (s/l) of 1.6 g L^{-1}).

m-PDA adsorption depended on the initial concentration. Increase in m-PDA concentration accelerated the diffusion m-PDA from the bulk solution onto adsorbent was due to higher concentration gradient [22]. The observed kinetics was modeled assuming that the rate of occupation of adsorption sites is proportional to the number of unoccupied sites (pseudo-first-order model) or the square of the number of unoccupied sites (pseudo-second-order model). Moreover, Elovich kinetic model, Weber and Morris intraparticle diffusion model, and Boyd model have also been used to test the dynamics of adsorption process. The prediction of the adsorption rate provided important information for designing batch adsorption systems. The derived rate constants together with statistical parameters are depicted in Table 2.

The regression coefficients (R^2) of the pseudo-first order model for m-PDA sorption were satisfactory (0.912–0.921) and the values of SE (0.359–0.458) and SSE (1.392–1.975) were low, suggesting a congruity of this model to the time-course sorption data. Moreover, the difference between experimental adsorption capacity (19.725–31.784 mg g⁻¹) and the one calculated from the model (12.51–25.14 mg g⁻¹) at equilibrium was marginal. Similar results were reported for reactive blue 5G sorption by activated carbon [23]. Suitability of experimental kinetic data to the pseudo-first order model confirmed the adsorption process governed by liquid film diffusion [24].

Generally, the pseudo-second-order equation was used to describe chemisorption involving valency forces through the sharing or exchange of electrons between the adsorbent and adsorbate as covalent forces and ion exchange [25]. In addition, the initial adsorption rate, h ($=k_2q_e^2$) can also be obtained from this model. In comparison, the pseudo-second-order model regression coefficient values were found to be higher, and ranged from 0.991 to 0.996, while SE and SSE values were lower and ranged from 0.048 to 0.052 and 0.001 to 0.003, respectively. The high R^2 and low SE and SSE values as well as the consonance between the experimental and predicted equilibrium sorption capacities confirmed compatibility to the pseudo-second-order model (Fig. 1). The adsorption of m-PDA onto activated carbon follows the pseudo-second-order model and hence, it can be presumed that more than onestep including chemisorption may be involved in the sorption process [26]. The values of the rate constant k_2 decreased with increase in initial m-PDA concentration while the initial adsorption rate, h , seemed to have an increasing trend with increasing initial m-PDA concentration (Table 2). This behavior can be ascribed to the increase in sorption driving force at higher concentration [27].

The characteristics of pseudo-second-order kinetic curve are useful to determine whether the m-PDA adsorption by activated carbon approaches equilibrium. The approaching equilibrium factor can be written as displayed in Eqs. (4) and (5) [23]:

$$k_2 q_e t_{\text{ref}} = \frac{R_W - 1}{R_W} \quad (4)$$

and

$$Q_t = \frac{T}{R_W(1 - T) + T} \quad (5)$$

where $T = t/t_{\text{ref}}$, R_W is known as an approaching equilibrium factor, t_{ref} is the longest operational time in an adsorption system and Q_t is the dimensionless factor, respectively. The R_W values in the adsorption of m-PDA on to activated carbon for the pseudo-second-order model are 0.008, 0.011, and 0.017 at initial concentrations of 50, 75, and 100 mg L⁻¹, respectively (Table 3). Similar R_W values were reported for adsorption of paraquat on activated clay ($R_W=0.017$) [22] and 4-nitro phenol on yellow bentonite ($R_W=0.01$) [28]. In general, R_W depended on the properties of solution, adsorbent, and adsorbate. The R_W values indicated that the characteristic adsorption curve (Fig. 3) approached pseudoequilibrium in the range $0.1 > R_W > 0.01$, which confirmed kinetic data were well represented by pseudo-second order model. The curvature of the adsorption curve increased as R_W reduced. The curvature of the adsorption process increased when $R_W=0.008$ while it decreased at a higher value of R_W (0.017), indicating that the removal of m-PDA from aqueous solution required larger amount of the activated carbon [25]. The relationship between the operating time for the adsorption of m-PDA by activated carbon and the extent of its adsorption is represented by this characteristic curve. These results are of paramount importance for effective engineering design under practical scenarios. When the sorption curve belonged to zone II, the relationship between operating time and amount of sorption is an important factor in engineering practice.

The second-order kinetic model has been used to describe the reactions between soil and soil mineral systems [29], but recently, this model has also been used for liquid phase adsorption systems [30,31]. Low values of R^2 (0.621–0.701) and high SE (6.758–8.682) and SSE (22.143–32.559), indicated that the second-order kinetic model explains the process kinetics very poorly in comparison with the pseudo-second-order model for m-PDA adsorption on to activated carbon.

Table 2
Parameters of kinetic models for m-PDA adsorption on activated carbon

Models		Initial concentration		
		$C_0 = 50 \text{ mg L}^{-1}$	$C_0 = 75 \text{ mg L}^{-1}$	$C_0 = 100 \text{ mg L}^{-1}$
q_e (Experimental)		19.725	23.561	31.784
<i>Pseudo-firstorder</i>	$q_t = q_e[1 - \exp(-k_1 t)]$			
k_1 (min^{-1})		0.078	0.069	0.0042
q_e		12.51	15.79	25.14
R^2		0.912	0.919	0.921
SE		0.458	0.389	0.359
SSE		1.975	1.625	1.392
<i>Pseudo-second order</i>	$q_t = \frac{k_2 q_e^2 t}{(1 + k_2 q_e t)}$			
q_e (mg g^{-1})		22.15	26.17	32.68
k_2 ($\text{g mg}^{-1} \text{min}^{-1}$)		0.018	0.011	0.006
h ($\text{mg g}^{-1} \text{min}^{-1}$)		8.831	7.532	5.334
R^2		0.991	0.996	0.992
SE		0.052	0.048	0.052
SSE		0.003	0.001	0.002
<i>Secondorder</i>	$q_t = \frac{C_0}{(C_0 k_{\text{SOR}} t + 1)}$			
k_{SOR} (min^{-1})		0.152	0.218	0.427
R^2		0.701	0.659	0.621
SE		6.758	7.514	8.682
SSE		22.143	28.192	32.559
<i>Elovich</i>	$q_t = (1/\beta_E) \cdot \ln(1 + \alpha_E \beta_E t)$			
α_E		25.27	40.26	55.15
β_E		0.034	0.041	0.053
R^2		0.848	0.929	0.824
SE		1.525	1.068	1.114
SSE		3.337	2.292	3.025
<i>Intraparticle diffusion</i>	$q_t = k_{\text{ip}} \sqrt{t} + c$			
k_{ip} ($\text{mg g}^{-1} \text{min}^{0.5}$)		56.19	57.45	57.12
R^2		0.983	0.992	0.987
SE		0.4123	0.3051	0.4074
SSE		1.2320	0.9022	0.1856
D_{IPD} ($\text{m}^2 \text{s}^{-1}$)		2.24×10^{-19}	3.08×10^{-19}	5.16×10^{-20}
<i>Boyd model</i>				
D_i ($\text{cm}^2 \text{s}^{-1}$)		2.047×10^{-9}	2.83×10^{-9}	3.527×10^{-9}
R^2		0.921	0.931	0.915
SE		0.728	0.529	0.603
SSE		2.562	1.634	2.432

Table 3
Adsorption kinetic behavior in the PSO model and equilibrium approaching factor (R_w)

R_w value	Type of kinetic curve	Approaching equilibrium level
$R_w = 1$	Linear	Not approaching equilibrium
$1 > R_w > 0.1$	Slightly curved	Approaching equilibrium
$0.1 > R_w > 0.01$	Largely curved	Well approaching equilibrium
$R_w < 0.01$	Pseudo-rectangular	Drastically approaching equilibrium

Further, the kinetic data were fitted to the Elovich (chemical reaction) mechanism assuming that the actual rate equation, which describes chemical adsorption solid surfaces are energetically heterogeneous [32].

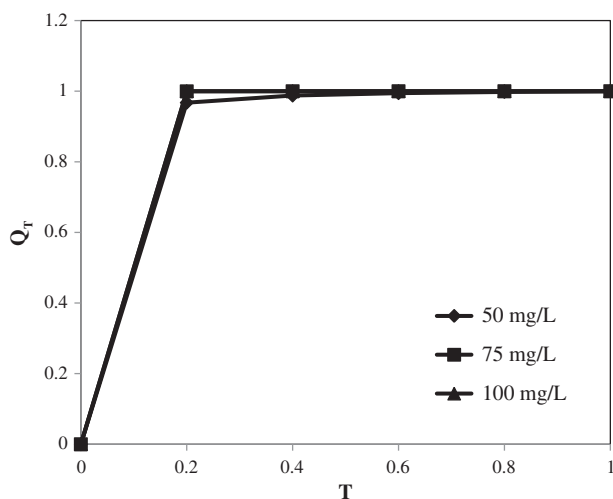


Fig. 3. Characteristic curves of pseudo-second-order kinetic model.

The R^2 (0.824–0.929), SE (1.068–1.525), and SSE (2.292–3.337) values revealed a moderate compatibility to the experimental kinetic data. With the increase in initial m-PDA concentration, the Elovich constants α_E and β_E increased showing that both the rate of chemisorption and the available sorption surface would increase. The moderate applicability of the simple Elovich equation for the present kinetic data revealed that active sites are heterogeneous in nature and exhibit different activation energies [32]. This supported the hypothesis that the heterogeneous sorption mechanism is likely to be responsible for the m-PDA uptake by activated carbon.

It may be concluded that out of the various kinetic models studied, the pseudo-second-order model was evidently more appropriate for kinetic modeling of time-course m-PDA adsorption data followed by pseudo-first-order and Elovich models.

3.3. Intraparticle diffusion (IPD) kinetic model

As the kinetic models like pseudofirst order, second-order, pseudo-second order, Elovich and Bhattacharya and Venkobachar kinetic models equations were not able to describe the adsorption mechanism, and also the rate-limiting steps in the adsorption process, the IPD model was used. Usually, the initial adsorption occurs on the adsorbent surface during batch experiments and there is a high probability of the adsorbate to diffuse into the interior pores of the adsorbent and hence, IPD emerges as the dominant process [33]. Ideally, a straight line is expected for the plot of solute sorbed against the square root of the contact time, where intraparticle diffusion is the rate-

determining step, while multilinearity represents different mechanisms involved in the sorption process [34]. The plot for this model gave two straight lines and the first incisive stage involved the sorption period of 0–90 min, which represents momentary adsorption or exterior surface adsorption (macropore diffusion), while the second stage included the sorption period of 80–240 min, representing gradual adsorption related to the rate limiting step (microand mesopore diffusion) (Figure not shown). The intraparticle diffusion, k_{ip} , values were obtained from the slope of the second linear portions of the plot of q_t vs. $t^{0.5}$ for various m-PDA concentrations. The intercept of the plot provided an estimation of the thickness of the boundary layer, i.e. the larger the intercept value, the greater was the boundary layer effect [25]. A high regression coefficients (R^2) (0.945–0.972), low SE (0.114–0.0247) and SSE (0.039–0.492) value suggested a significant relationship between q and $t^{0.5}$ all the three tested concentrations of m-PDA. The intraparticle rate constant values (k_{ip}) increased from 0.326 to 0.492 $\text{mg g}^{-1} \text{min}^{0.5}$ with the increase in the initial concentration of m-PDA from 50 to 100 mg L^{-1} (Table 1). The increase in k_{ip} values with increasing initial m-PDA concentration can be explained by the growing effect of driving force resulted in reducing the diffusion of m-PDA in the boundary layer and enhancing the diffusion in the solid [35]. Moreover, the variation of intra-particle diffusion rate constant is a normal phenomenon as reported in various studies [25]. The value of intercept, C , increased (14.263–23.654) with increasing concentration of m-PDA (50–100 mg L^{-1}). This happened because a high m-PDA concentration seemed to have provided better driving force to external mass transfer process. On the other hand, C was $\neq 0$ at all the test conditions, thereby suggesting that intraparticle diffusion was not the rate-limiting step and external mass transfer has also played an important role in m-PDA sorption by activated carbon [36]. The diffusion coefficients for the intraparticle transport of m-PDA within the pores of activated carbon particles have been calculated by Eq. (6) [37]:

$$D_{IPD} = \frac{0.03r_0^2}{t_{1/2}} \quad (6)$$

The average radius of the adsorbent particles and the time required to change half of adsorption of m-PDA were denoted by r_0 (m) and $t_{1/2}$ (min), respectively. The half-adsorption time ($t_{1/2}$) can be calculated from the equilibrium concentration and the PSO rate constant values [38]. The calculated D_{IPD} values ranged from 7.52×10^{-19} to $5.16 \times 10^{-20} \text{ m}^2 \text{ s}^{-1}$ for three

concentrations studied indicating that IPD does not account for the rate-controlling step of m-PDA [39]. Though, the IPD kinetic model represents the adsorption of m-PDA from aqueous solution by activated carbon, it cannot be considered as the rate controlling step.

3.4. Boyd plot

The kinetic data were further analyzed by Boyd film-diffusion model for evaluating the contribution of film resistance and to determine the actual rate controlling step involved in the sorption of m-PDA on to activated carbon. Boyd model assumes that the main resistance to diffusion is within the boundary layer surrounding the adsorbent and is expressed as [40]:

$$F = 1 - \frac{6}{\Pi^2} \sum_{n=1}^{\infty} \frac{1}{n^2} \exp(-n^2 Bt) \quad (7)$$

where F is the fractional attainment of equilibrium, at different times, t , and Bt is the function of F .

$$F = \frac{qt}{qe} \quad (8)$$

B , can be used to calculate the effective diffusion coefficient, D_i ($\text{cm}^2 \text{s}^{-1}$), from the equation:

$$B = \frac{\Pi^2 D_i}{r_0^2} \quad (9)$$

where r_0 is the radius of the adsorbent particle and n is the integer that defines the infinite series solution. Bt is given by the equation:

$$Bt = -0.4977 - \ln(1 - F) \quad (10)$$

Thus, the value of Bt was computed for each value of F , and then plotted against time to form the so-called Boyd plot (Figure not shown). The linearity of Boyd plot was employed to distinguish between sorption controlled by film diffusion and particle diffusion [41]. A straight line passing through the origin is indicative of adsorption processes governed by particle-diffusion mechanisms. If the plot is nonlinear or linear but does not pass through the origin, then it is concluded that the process is controlled by film-diffusion [42]. The plots in the present study were neither linear nor passed through the origin at various initial concentrations, indicating the film diffusion-

controlled mechanism. In general, external transport is the rate-limiting step in systems, which have poor mixing, dilute concentration of adsorbate, small particle size, and high affinity of adsorbate for biosorbent. However, the intraparticle step limits the overall transfer for those systems that have high concentration of adsorbate, good mixing, large particle size of sorbent and low affinity of adsorbate for sorbent [43]. In the present study, the strong external resistance which hinder the external mass transfer may be owing to the poor mixing (agitation speed 140 rpm), low concentration of adsorbate (initial concentration, 50, 75 and 100 mg L^{-1}), and small particle sizes of activated carbon (250 μm). Besides, the m-PDA displays higher affinity for the activated carbon, which results in low internal resistance. Because the overall rate of sorption will be controlled by the slowest step, so that the external mass transport (film diffusion) mainly governs the intraparticle diffusion. Similar results were reported in the literature [44,45].

3.5. Adsorption equilibrium

Analysis of equilibrium data is essential for deriving an equation that can be used to design and optimize an operating procedure for adsorption process. To examine the relationship between adsorption of m-PDA and aqueous concentration at equilibrium, various adsorption isotherm models including the Langmuir [46], Freundlich [47], and Redlich–Peterson [48] were employed for fitting the data in the present work. The isotherm constants along with statistical parameters at various temperatures are presented in Table 4.

The Langmuir model used to estimate the maximum metal uptake value where it could not be reached in the experiments and it contained two important parameters of the adsorption system (K_L and b). The regression coefficients demonstrated that the adsorption of m-PDA matched better with the Redlich–Peterson ($R^2 > 0.982$) and Langmuir isotherms ($R^2 > 0.939$) than the Freundlich isotherm. The values of maximum adsorption capacity (K_L) and the coefficient attributed to the affinity between the sorbent and sorbate in the Langmuir model increased from 39.904 to 41.893 mg g^{-1} and 0.046 to 0.066 L mg^{-1} , respectively, with increase in temperature from 293 to 323 K, indicating that the adsorption is endothermic process. The increasing trend in adsorption capacity with temperature may be due to the atrophy of sorptive forces between the active sites of the activated carbon and m-PDA. The separation factor, R_L ($0 < R_L < 1$), indicated that the activated carbon was a suitable adsorbent for sorption of m-PDA from aqueous solutions.

Table 4
Isotherm parameters for m-PDA adsorption on activated carbon at various temperatures

Models		Temperature (K)			
		293	303	313	323
Experimental q_e		32.156	33.171	34.807	35.328
Langmuir	$q_e = \frac{bk_L C_e}{1+bC_e}$ $R_L = \frac{1}{1+bC_0}$				
b (L mg ⁻¹)		0.046	0.051	0.055	0.066
k_L (mg g ⁻¹)		39.904	40.322	41.027	41.893
R_L		0.241	0.355	0.412	0.601
R^2		0.939	0.971	0.983	0.990
SE		0.361	0.314	0.285	0.249
SSE		0.653	0.493	0.407	0.310
Freundlich	$q_e = K_F C_e^{\frac{1}{n}}$				
K_F (L g ⁻¹)		43.268	54.344	61.307	72.424
N		2.7367	3.013	3.232	3.945
R^2		0.801	0.825	0.807	0.845
SE		0.437	0.365	0.414	0.249
SSE		0.924	0.737	0.961	0.413
Redlich–Peterson	$q_e = \frac{K_{RP} C_e^{\gamma_{RP}}}{1+a_{RP} C_e^{\gamma_{RP}}}$				
K_{RP} (mg g ⁻¹)		34.936	35.054	36.236	37.128
a_{RP} (L mg ⁻¹)		0.486	0.524	0.547	0.594
γ_{RP}		0.872	0.846	0.913	0.938
R^2		0.982	0.995	0.989	0.992
SE		0.418	0.165	0.342	0.207
SSE		0.714	0.225	0.524	0.485

The Freundlich isotherm is originally empirical in nature and has been used widely to suit experimental data of liquid phase sorption [43]. The magnitude of n in this model can quantify the favorability of adsorption and the degree of heterogeneity of the activated carbon surface. The values of n were found in this study to be larger than unity, indicating that the m-PDA is favorably adsorbed by activated carbon at various temperatures. Statistically, the Freundlich model gave a satisfactory shape to the experimental data with moderate R^2 (0.801–0.845) and low SE (0.249–0.437) and SSE (0.413–0.961) values.

The equilibrium adsorption data were well adequately represented by the Langmuir and Freundlich isotherms, respectively. The Langmuir type isotherm suggested surface homogeneity of the adsorbent, while the Freundlich type adsorption isotherm is an indication of surface heterogeneity. This may be due to both the homogeneous and heterogeneous distributions of active sites on the activated carbon surface. The adsorption properties of the activated carbon are thus, likely to be complex and would involve more than one mechanism [49].

Among the isotherm models having three parameters, the Redlich–Peterson has been most frequently employed in liquid phase adsorption systems and

has the features of the Langmuir and Freundlich isotherms. It approaches the Freundlich model at a high concentration and is in accordance with the low concentration limit of the Langmuir equation. The Redlich–Peterson model correctly simulates the adsorption isotherms of m-PDA-activated carbon system at various temperatures (Fig. 4). The regression coefficients (R^2) were very high (0.982–0.995), and with low values of SE (0.165–0.548) and SSE (0.225–0.714) for tested systems. The γ_{RP} values ranged from 0.872 to 0.938 i.e. the data can preferably to be fitted with the Langmuir. This is confirmed by the satisfactory fit of the data to the Langmuir model.

3.6. Multi-stage batch design model

A wastewater treatment process consisting of a series of adsorption and desorption stages can be considered as a multi-stage equilibrium operation, and an adsorption isotherm is generally used to design a multi-stage adsorption/regeneration system [50,51]. The design objective is to reduce the m-PDA concentration in the feed (of volume V) from C_0 to C_n (mg L⁻¹), reusing the adsorbent (of mass W) in each adsorption stage after desorption (Fig. 5). The dye

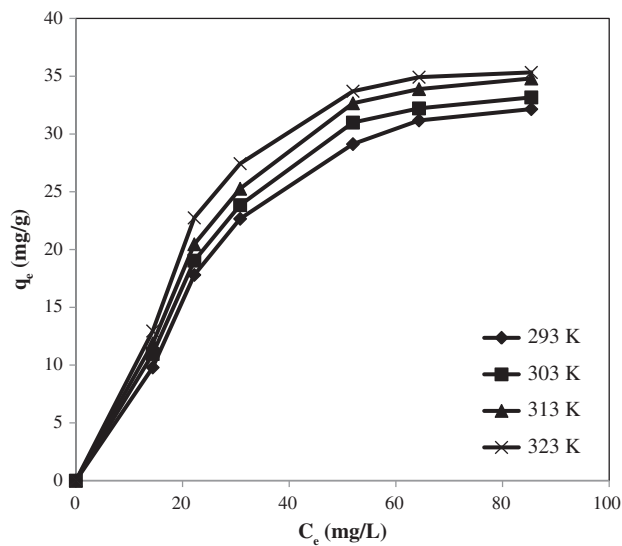


Fig. 4. Experimental (legends) and the Redlich–Peterson (lines) isotherms for sorption of m-PDA by activated carbon at various temperatures (pH 7.0 and solid to liquid ratio (s/l) of 1.6 g L^{-1}).

mass balance for batch adsorber system (n) can be written as:

$$VC_{n-1} + Wq_r = VC_n + Wq_n \quad (11)$$

Assuming that the desorption efficiency of the studied system was 100%, so $q_r = q_0 = 0$, and the Eq. (11) becomes:

$$V(C_{n-1} - C_n) = Wq_n \quad (12)$$

Adsorption isotherm data were found to fit the Langmuir model for adsorption of m-PDA on AC. Thus, the Langmuir equation can be used to for q_n in Eq. (12):

$$\frac{W}{V} = \frac{C_{n-1} - C_n}{\left(\frac{bk_1 C_n}{(1+bC_n)}\right)} \quad (13)$$

Eq. (13) can be solved to give:

$$C_n = \frac{-\left(\frac{W}{V}bk_L - bC_{n-1}\right) \pm \sqrt{\left(\frac{W}{V}bk_L - bC_{n-1}\right)^2 + 4bC_{n-1}}}{2b} \quad (14)$$

For the first adsorption cycle ($n = 1$), C_{n-1} in Eq. (14) is replaced by the initial concentration C_0 . Eq. (14) was used to determine the concentration after each stage of treatment for a given feed concentration C_0 and weight of adsorbent (W) using the Langmuir isotherm constants. The amount of adsorbent (W) was estimated for a five-stage-adsorption-desorption system to achieve m-PDA removal ranging from 10 to 99% with various initial concentrations ($25\text{--}150 \text{ mg L}^{-1}$) (Fig. 6). The amount of adsorbent increased linearly with the percentage m-PDA removal up to elimination of around 90–95%. This may be attributed to the fact that as adsorbent approaches its maximum loading in each of the adsorption cycles, the amount of m-PDA removed per gram of adsorbent was approximately constant. However, the m-PDA concentration in the final adsorption stage should be low so that the adsorbent used in this stage will not be fully saturated to achieve high removal.

An experimental study of a five-stage adsorption-desorption process was conducted for the adsorption of m-PDA with an initial concentration of 50 mg L^{-1} onto AC for validation of the model. The value of the percentage removal achieved after each stage obtained from the model and the experiment was compared (Fig. 7). The percentage removal of m-PDA was increased from 19 to 93% in stages 1–5, and there was good consonance between the experimental data and the model.

3.7. Adsorption thermodynamics

The thermodynamic parameters, such as the standard Gibbs free energy ΔG° (kJ mol^{-1}), standard enthalpy change ΔH° (J mol^{-1}), and standard entropy change ΔS° ($\text{J mol}^{-1} \text{ K}$) were calculated using the Eqs. (15–17):

$$\ln K_c = \frac{\Delta S^\circ}{R} - \frac{\Delta H^\circ}{RT} \quad (15)$$

$$\Delta G^\circ = -RT \ln K_c \quad (16)$$

$$K_c = \frac{y_{\text{ads}}}{y_e} = \frac{\gamma_{\text{ads}} C_{\text{ads}}}{\gamma_e C_e} \quad (17)$$

where K_c is the thermodynamic distribution coefficient, T is the absolute temperature (K), R is the gas constant ($\text{J mol}^{-1} \text{ K}$), C_{ads} is the amount of m-PDA adsorbed on the adsorbent (mg g^{-1}), C_e is the equilibrium concentration of the m-PDA in the

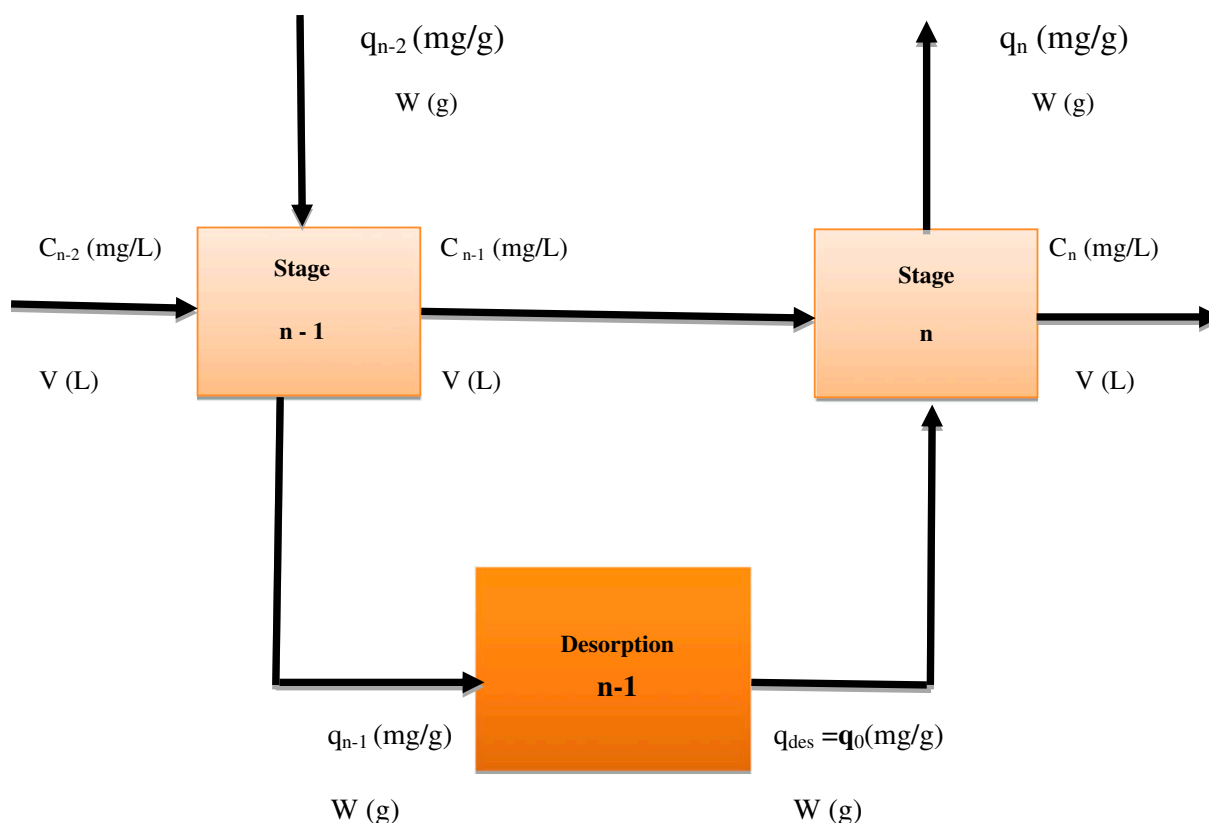


Fig. 5. Schematic diagram of two stages in a multi-stage batch adsorption/desorption system.

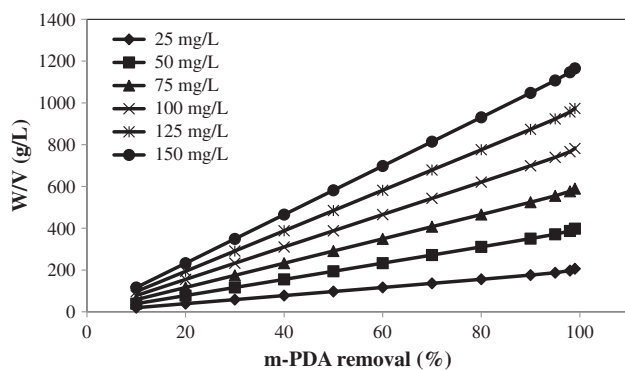


Fig. 6. The adsorbent dose required as a function of the m-PDA removal for a range of initial m-PDA concentrations using a five stage batch adsorption–desorption system.

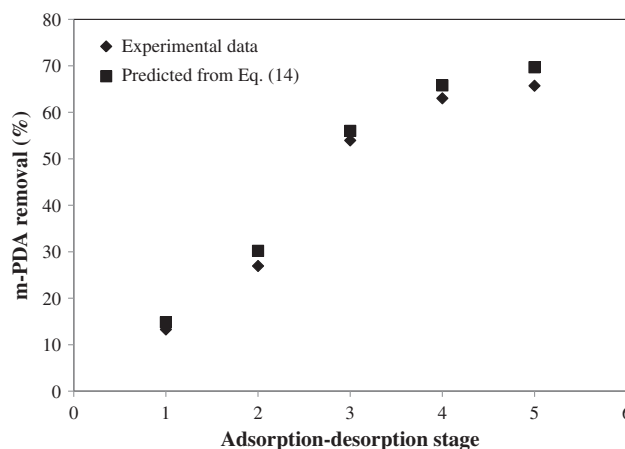


Fig. 7. Performances of batch adsorption–desorption for removal of m-PDA using activated carbon with five stages adsorption and desorption.

solution (mg L^{-1}), y_{ads} is the activity of adsorbed m-PDA, y_e is the activity of m-PDA in solution at equilibrium, γ_{ads} is the activity coefficient of adsorbed m-PDA and γ_e is the activity coefficient of m-PDA. The expression of K_c can be simplified by assuming that the concentration in the solution approaches zero resulting in $C_{\text{ads}} \rightarrow 0$ and $C_e \rightarrow 0$, and the

activity coefficients approach unity at very low concentrations [52].

An increase in temperature (293–323 K) resulted in an increased rate of m-PDA adsorption indicated that the process was endothermic (Fig. 3). The van't Hoff

plot of $\ln K_c$ vs. $1/T$ (Figure not shown) resulted in a straight line with a slope of ΔH° (J mol^{-1}) and an intercept of ΔS° ($\text{J mol}^{-1} \text{K}$). Consequently, the adsorption thermodynamics parameters were calculated by the above equation (Table 5). The overall ΔG° during the adsorption was negative for the range of temperatures investigated, and the degree of spontaneity of the reaction increases with increasing temperature. The positive value of ΔH° confirmed the endothermic nature of the adsorption also supported by the increase in value of AC uptake with the rise in temperature. As the temperature increased, more active sites upon the AC were available, which resulted in an enhancement in adsorption due to the increase in surface activity and kinetic energy of the m-PDA molecules. The experimental enthalpy change was below 40 kJ mol^{-1} , which implied that physisorption dominates the adsorption of m-PDA onto AC [53]. The positive value of ΔS° ($21.53 \text{ J K mol}^{-1}$) corresponds to an increase in the randomness at the solid–solute interface, which indicates that the affinity of m-PDA toward the AC was high. Similar results were reported in the literature [54,55].

3.8. Reuse of the adsorbent

Desorption experiments were performed to investigate the possibility of the regeneration of the activated carbon as it enhanced the economic value of adsorption process. The desorption efficiency (%) was defined as the ratio of the amount of the m-PDA desorbed to the amount of the m-PDA adsorbed. About 98% adsorbed m-PDA was desorbed from the spent adsorbent using 5% acetone, and the adsorbent could be regenerated and reused at least five times without a significant loss (around 4–8%) of the sorption capacity. Even after five cycles of adsorption–desorption cycles, no loss of adsorbent was observed, which made the adsorbent most suitable for the industrial applications. These results indicated that the m-PDA adsorption on activated carbon was reversible and relatively easy for the adsorbed m-PDA to be desorbed from the samples.

3.9. FTIR and SEM analysis

FTIR analysis was performed to confirm the presence of various functional groups, such as hydroxyl, carboxyl, sulfhydryl, sulfonate, etc. above groups in activated carbon and to elucidate the nature of the AC–m-PDA interaction. The FTIR spectra of unloaded and m-PDA loaded form of AC in the range of $400\text{--}4,000 \text{ cm}^{-1}$ were taken (Fig. 8). The FTIR spectrum of activated carbon showed several distinct and sharp absorptions at $3,434 \text{ cm}^{-1}$ (indicative of primary amide, N–H group), $2,924 \text{ cm}^{-1}$ (indicative of –CH stretching), $2,617 \text{ cm}^{-1}$ (indicative of carboxylic acids, O–H group), $2,362 \text{ cm}^{-1}$ (indicative of N–H stretching of amide), $1,629 \text{ cm}^{-1}$ (indicative of amide I band of amide bond in *N*-acetyl glucosamine polymer or of the protein peptide bond), $1,384 \text{ cm}^{-1}$ (indicative of nitro group, N=O) and the band at $1,022 \text{ cm}^{-1}$ (indicative of ether group, C–O). The FT-IR spectra of activated carbon after adsorption of m-PDA indicated shift in the intensity of bands from $3,434$ to $3,439 \text{ cm}^{-1}$, $2,924$ to $2,918 \text{ cm}^{-1}$, $2,362$ to $2,357 \text{ cm}^{-1}$, $1,629$ to $1,635 \text{ cm}^{-1}$, and $1,384$ to $1,380 \text{ cm}^{-1}$. The changes in the spectra showed involvement of amide groups, O–H group of carboxylic acids, and nitro groups in sorption of m-PDA.

SEM images of activated carbon before (Fig. 9(a)) and after adsorption (Fig. 9(b)) of m-PDA clearly distinguish two cases. The surface of activated carbon before adsorption showed an uneven surface and porous structure. Pores and cavities of various dimensions are also clearly evident on the surface and are highly heterogeneous. The heterogeneous pores and cavities provided a large exposed surface area for the adsorption of m-PDA, and indicate that there was a good possibility for the m-PDA molecules to be trapped and adsorbed onto the surface of the activated carbon. These cavities are large enough to allow the m-PDA molecules to penetrate and interact therein with the surface groups. After adsorption of m-PDA, the pores were filled and they appear to be prominently swollen. This observation indicates that m-PDA is adsorbed to the functional groups present inside the pores.

Table 5

Thermodynamic parameters for m-PDA adsorption onto activated carbon at various temperatures

Temperature (K)	ΔG° (kJ mol^{-1})	ΔH° (J mol^{-1})	ΔS° (J (mol K)^{-1})
293	–1.21	13.60	21.53
303	–1.09		
313	–0.97		
323	–0.82		

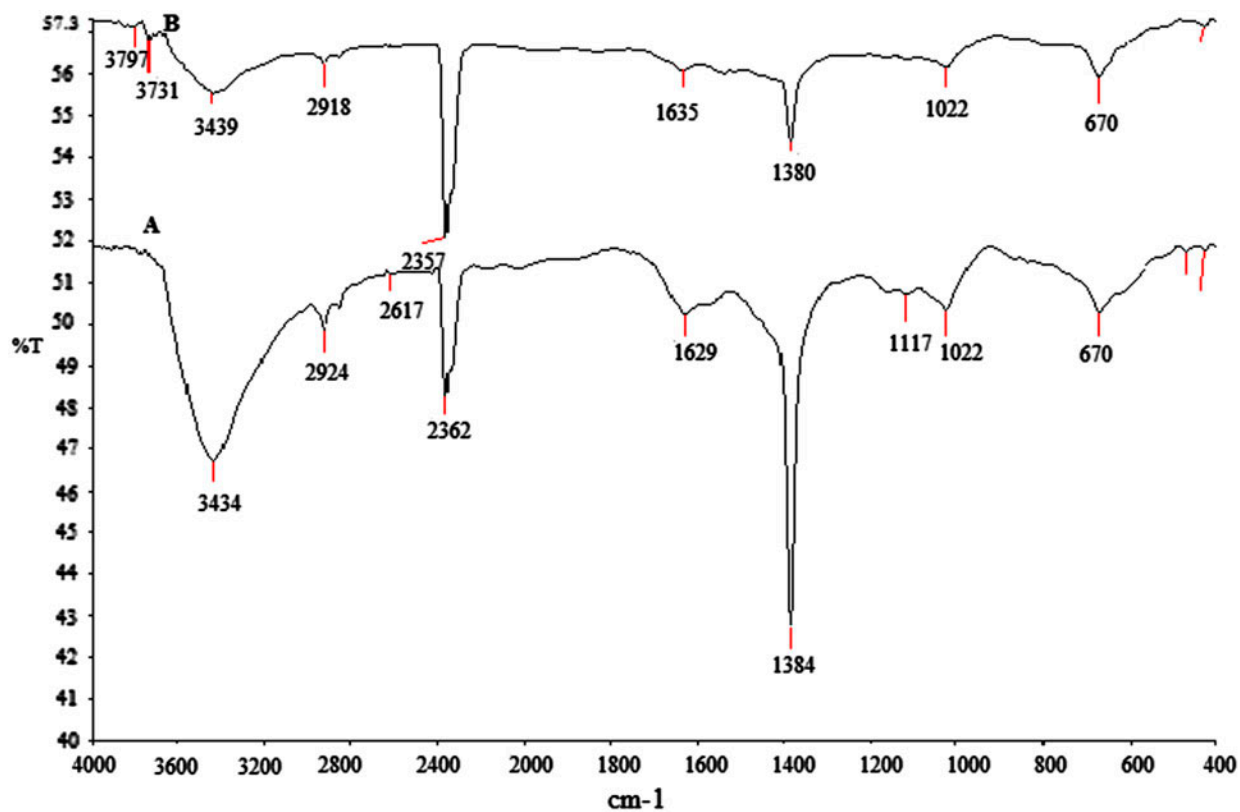


Fig. 8. FTIR spectra of activated carbon (A), and m-PDA loaded activated carbon (B).

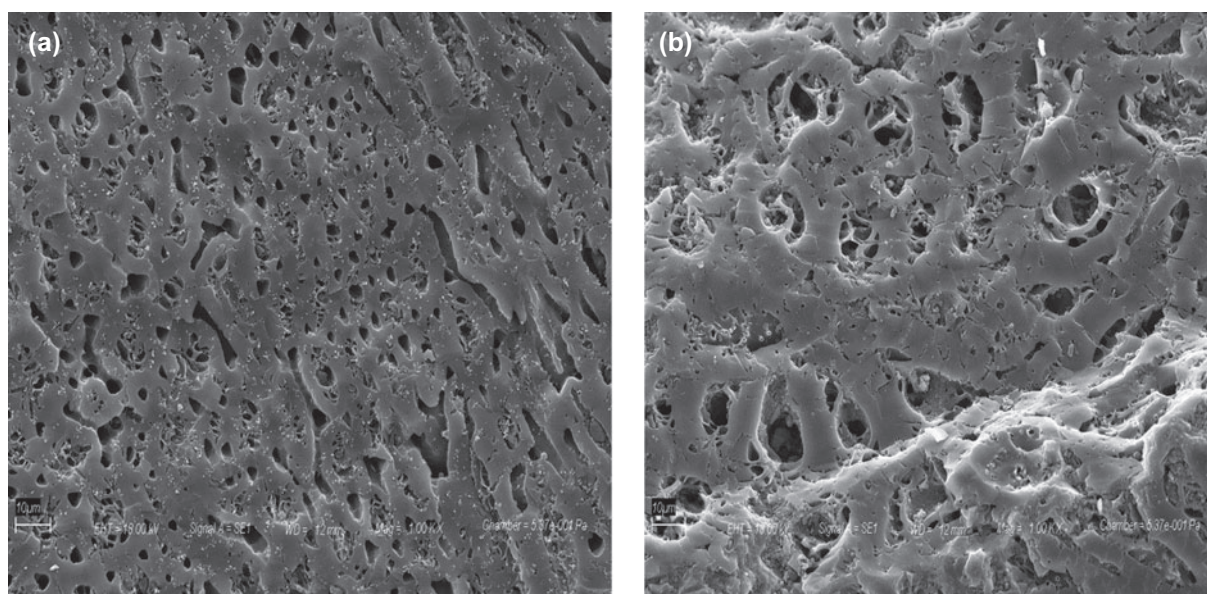


Fig. 9. SEM of activated carbon (a), and m-PDA loaded activated carbon (b).

4. Conclusions

The removal of m-PDA from aqueous solutions using activated carbon was systematically studied. The adsorption process was pH dependent and the optimum pH for maximum adsorption was 7.0. Adsorption kinetics was well described by the pseudo-second-order rate equation and the equilibrium isotherms belong to the Redlich–Peterson model. The Weber–Morris intraparticle diffusion model suited well to the time-course m-PDA sorption data, thus implying involvement intra-particle diffusion processes in sorption of m-PDA by activated carbon. However, the Boyd kinetic expression clearly showed that the film diffusion was the dominant process. A model was developed to predict the dose of adsorbent required to achieve a range of m-PDA removals for a given number of adsorption–desorption cycles, based on the Langmuir isotherm data. The model was found to be in excellent consonance with the experimental results obtained for five stages of adsorption–desorption. The adsorption capacity increased with the corresponding rise in temperature indicating that the adsorption was an intrinsic and endothermic process. This was also supported by the thermodynamic parameters calculated at different temperatures. The FTIR spectra of raw and m-PDA loaded activated carbon indicated that amide, carboxylic acid and nitro groups were major binding sites of m-PDA.

Acknowledgements

The authors wish to express their sincere thanks to Professor Bhavanath Jha, Discipline co-ordinator of Marine Biotechnology and Ecology for his valuable suggestions. Thanks are also due to Mr. Harshad Brahbhatt for HPLC analysis.

References

- [1] P.E. Vogt, J.J. Gerialis, Ullmann's Encyclopedia of Industrial Chemistry, fifth ed., vol. A2, VCH, Weinheim, 1985, p. 37.
- [2] E. Gonzalez-Pradas, M. Villafranca-Sanchez, M.D. Urena-Amate, F. Del Rey-Bueno, A. Garcia-Rodriguez, Removal of aromatic amines from water by montmorillonite-(cerium or zirconium) phosphate crosslinked compounds, *J. Environ. Qual.* 28 (2009) 115–120.
- [3] O. Kirk, Encyclopedia of Chemical Technology, third ed., vol. 2, Wiley Interscience, New York, NY, 1978, p. 272.
- [4] M.S. Reisch, Better times ahead for U.S. dye producers, *Chem. Eng. News* 66 (1988) 7–14.
- [5] S. Chen, Sorption and Desorption Behavior of Aromatic Amine in Solvent-Sediment Systems, PhD Thesis, Rensselaer Polytechnic Institute, New York, NY, 2007.
- [6] H. Rojas, G. Borda, M. Brijaldo, P. Reyes, J. Valencia, Kinetics and mechanism of the hydrogenation of m-dinitrobenzene to m-phenylenediamine, *Reac. Kinet. Mech. Cat.* 105 (2012) 271–284.
- [7] R.L. Mayer, Aromatic amines and azo-dyes in allergy and cancer, *J. Invest. Dermatol.* 10 (1948) 389–396.
- [8] H. Amo, M. Matsuyama, H. Amano, C. Yamada, M. Kawai, N. Miyata, M. Nakadate, Carcinogenicity and toxicity study of m-phenylenediamine administered in the drinking-water to (C57BL/6×C3H/He) F1 mice, *Food Chem. Toxicol.* 26 (1988) 893–897.
- [9] A.M. Klibanov, B. Mass, Removal of Combined Organic Substances from Aqueous Solutions, US Patent 4623465, 1989.
- [10] C.-C. Su, L.V. Panopio, G.L. Peralta, M.-C. Lu, Application of Fered-Fenton process for m-phenylenediamine degradation, *J. Environ. Sci. Health A Tox. Hazard. Subst. Environ. Eng.* 48 (2013) 1012–1018.
- [11] C. Moreno-Castilla, Adsorption of organic molecules from aqueous solutions on carbon materials, *Carbon* 42 (2004) 83–94.
- [12] R.A. Rao, M. Ajmal, R. Ahmad, B.A. Siddiqui, Adsorption behaviour of some aromatic amines on pyrolusite and activated carbon and recovery of beta naphthylamine from water sample, *Environ. Monit. Assess.* 68 (2001) 235–247.
- [13] H.A. Arafat, F. Ahnert, N.G. Pinto, On the adsorption of aromatics on oxygenated activated carbon in non-aqueous adsorption media, *Sep. Sci. Technol.* 39 (2004) 43–62.
- [14] E. Yilmaz, S. Memon, M. Yilmaz, Removal of direct azo dyes and aromatic amines from aqueous solutions using two beta-cyclodextrin-based polymers, *J. Hazard. Mater.* 174 (2010) 592–597.
- [15] Y.S. Al-Degs, M.I. El-Barghouthi, A.H. El-Sheikh, G.M. Walker, Effect of solution pH, ionic strength, and temperature on adsorption behavior of reactive dyes on activated carbon, *Dyes Pigm.* 77 (2008) 16–23.
- [16] Y.-H. Kim, B. Lee, K.-H. Choo, S.-J. Choi, Adsorption characteristics of phenolic and amino organic compounds on nano-structured silicas functionalized with phenyl groups, *Microporous Mesoporous Mater.* (2013), doi: 10.1016/j.micromeso.2013.10.017.
- [17] D.D. Perrin, B. Dempsey, E.P. Serjeant, pKa Prediction for Organic Acids and Bases, Chapman and Hall, London, 1981.
- [18] J. Mattson, H. Mark, Activated Carbon: Surface Chemistry and Adsorption from Solution, Marcel Dekker, Inc., New York, NY, 1971.
- [19] Y. Leon, C. Leon, J. Solar, V. Calemma, L. Radovic, Evidence for the protonation of basal plane sites on carbon, *Carbon* 30 (1992) 797–811.
- [20] G. Newcombe, M. Drikas, Adsorption of NOM activated carbon: Electrostatic and non-electrostatic effects, *Carbon* 35 (1997) 1239–1250.
- [21] D.M. Ruthven, Principles of Adsorption and Adsorption Processes, Wiley, New York, NY, 1984.
- [22] W.T. Tsai, H.C. Hsu, T.Y. Su, K.Y. Lin, C.M. Lin, Adsorption characteristics of bisphenol-A in aqueous solutions onto hydrophobic zeolite, *J. Colloid Interface Sci.* 299 (2006) 513–519.
- [23] A. Rathinam, B. Maharshi, S.K. Janardhanan, R. Jonnalagadda, B.U. Nair, Biosorption of cadmium metal ion from simulated wastewater using *Hypnea*

- valentiae biomass: A kinetic and thermodynamic study, *Bioresour. Technol.* 101 (2010) 1466–1470.
- [24] V.P. Vinod, T.S. Anirudhan, Sorption of tannic acid on zirconium pillared clay, *J. Chem. Technol. Biotechnol.* 77 (2002) 92–101.
- [25] F.-C. Wu, R.-L. Tseng, S.-C. Huang, R.-S. Juang, Characteristics of pseudo-second-order kinetic model for liquid-phase adsorption: A mini-review, *Chem. Eng. J.* 151 (2009) 1–9.
- [26] X.-D. Xin, J. Wang, H.-Q. Yu, B. Du, Q. Wei, L.-G. Yan, Removal of o-nitrobenzoic acid by adsorption on to a new organoclay: Montmorillonite modified with HDTMA microemulsion, *Environ. Technol.* 32 (2011) 447–454.
- [27] T. Maiyalagan, S. Karthikeyan, Film-pore diffusion modeling for sorption of azo dye on to exfoliated graphitic nanoplatelets, *Indian J. Chem. Technol.* 20 (2013) 7–14.
- [28] Z. Yaneva, B. Koumanova, Comparative modelling of mono-and dinitrophenols sorption on yellow bentonite from aqueous solutions, *J. Colloid Interface Sci.* 293 (2006) 303–311.
- [29] R. Griffin, J. Jurinak, Kinetics of the phosphate interaction with calcite, *Soil Sci. Soc. Am. J.* 38 (1974) 75–79.
- [30] K.G. Varshney, A.A. Khan, U. Gupta, S.M. Maheshwari, Kinetics of adsorption of phosphamidon on antimony(V) phosphate cation exchanger evaluation of the order of reaction and some physical parameters, *Colloid Surf. Physicochem. Eng. Aspect.* 113 (1996) 19–23.
- [31] M. Mahramanlioglu, I. Kizilcikli, I. Bicer, Adsorption of fluoride from aqueous solution by acid treated spent bleaching earth, *J. Fluorine Chem.* 115 (2002) 41–47.
- [32] S. Chien, W. Clayton, Application of Elovich equation to the kinetics of phosphate release and sorption in soils, *Soil Sci. Soc. Am. J.* 44 (1980) 265–268.
- [33] W. Weber, J. Morris, Kinetics of adsorption on carbon from solution, *J. Sanit. Eng. Div. Am. Soc. Civ. Eng.* 89 (1963) 31–60.
- [34] Y.S. Ho, G. McKay, A comparison of chemisorption kinetic models applied to pollutant removal on various sorbents, *Process Saf. Environ. Prot.* 76 (1998) 332–340.
- [35] I.D. Mall, V.C. Srivastava, N.K. Agarwal, Removal of orange-G and methyl violet dyes by adsorption onto bagasse fly ash-kinetic study and equilibrium isotherm analyses, *Dyes Pigm.* 69 (2006) 210–223.
- [36] J. Ma, Y. Jia, Y. Jing, Y. Yao, J. Sun, Kinetics and thermodynamics of methylene blue adsorption by cobalt-hectorite composite, *Dyes Pigm.* 93 (2012) 1441–1446.
- [37] A.K. Bhattacharya, C. Venkobbar, Removal of cadmium by low cost adsorbents, *J. Environ. Eng.* 110(1) (1984) 110–122.
- [38] R. Han, P. Han, Z. Cai, Z. Zhao, M. Tang, Kinetics and isotherms of neutral red adsorption on peanut husk, *J. Environ. Sci.* 20 (2008) 1035–1041.
- [39] L. Michelsen, P. Gideon, E. Pace, L. Kutal, Removal of soluble Hg from water by complexing techniques, *U. S. D. I. Office Water Res. Tech. Bull.* 74 (1975).
- [40] G. Boyd, A. Adamson, L. Myers Jr, The exchange adsorption of ions from aqueous solutions by organic zeolites. ii. Kinetics, *J. Am. Chem. Soc.* 69 (1947) 2836–2848.
- [41] R. Djeribi, O. Hamdaoui, Sorption of copper(II) from aqueous solutions by cedar sawdust and crushed brick, *Desalination* 225 (2008) 95–112.
- [42] D. Mohan, K.P. Singh, Single- and multi-component adsorption of cadmium and zinc using activated carbon derived from bagasse—An agricultural waste, *Water Res.* 36 (2002) 2304–2318.
- [43] V. Vadivelan, K.V. Kumar, Equilibrium, kinetics, mechanism, and process design for the sorption of methylene blue onto rice husk, *J. Colloid Interface Sci.* 286 (2005) 90–100.
- [44] K.P. Singh, D. Mohan, S. Sinha, G.S. Tondon, D. Gosh, Color removal from wastewater using low-cost activated carbon derived from agricultural waste material, *Ind. Eng. Chem. Res.* 42 (2003) 1965–1976.
- [45] J. Aguilar-Carrillo, F. Garrido, L. Barrios, M.T. Garcya-Gonzalez, Biosorption of As, Cd and Tl as influenced by industrial by-products applied to an acidic soil: Equilibrium and kinetic experiments, *Chemosphere* 65 (2006) 2377–2387.
- [46] I. Langmuir, The constitution and fundamental properties of solids and liquids. I. Solids, *J. Am. Chem. Soc.* 38 (1916) 2221–2295.
- [47] H.M.F. Freundlich, Uber die adsorption in losungen, *Z Phys. Chem. (Leipzig)* 57A (1906) 385–470.
- [48] O. Redlich, D.L. Peterson, A useful adsorption isotherm, *J. Phys. Chem.* 63 (1959) 1024–1026.
- [49] Y. Yang, D. Jin, G. Wang, D. Liu, X. Jia, Y. Zhao, Biosorption of Acid Blue 25 by unmodified and CPC-modified biomass of *Penicillium* YW01: Kinetic study, equilibrium isotherm and FTIR analysis, *Colloids Surf., B* 88 (2011) 521–526.
- [50] E.I. Unuabonah, B.I. Olu-Owolabi, D. Okoro, K.O. Adebowale, Comparison of two-stage sorption design models for the removal of lead ions by polyvinyl-modified Kaolin clay, *J. Hazard. Mater.* 171 (2009) 215–221.
- [51] M. Ozacar, I.A. Sengil, Equilibrium data and process design for adsorption of disperse dyes onto alunite, *Environ. Geol.* 45 (2004) 762–768.
- [52] J.W. Biggar, M.W. Cheung, Adsorption of picloram (4-amino-3,5,6-trichloropicolinic acid) on Panoche, Ephrata, and Palouse soils-thermodynamic approach to adsorption mechanism, *Soil Sci. Soc. Am. J.* 37 (1973) 863–868.
- [53] N.C. Feng, X.Y. Guo, S. Liang, Adsorption study of copper(II) by chemically modified orange peel, *J. Hazard. Mater.* 164 (2009) 1286–1292.
- [54] M. Barkat, D. Nibou, S. Chearouche, A. Mellah, Kinetics and thermodynamics studies of chromium (VI) ions adsorption onto activated carbon from aqueous solutions, *Chem. Eng. Process.* 48 (2009) 38–47.
- [55] Z. Ren, L. Shao, G. Zhang, Adsorption of phosphate from aqueous solution using an iron-zirconium binary oxide sorbent, *Water Air Soil Pollut.* 223 (2012) 4221–4231.